2021

Plasma-Treated Water Affects Listeria Monocytogenes Vitality and Biofilm Structure

Oliver Handorf
University of Greifswald, oliver.handorf@inp-greifswald.de

Viktoria Isabella Pauker
University of Greifswald

Thomas Weihe
Leibniz Institute for Plasma Science and technology (INP)

See next page for additional authors

Recommended Citation

Handorf, O., Pauker, V.I. & Weihe, T. (2021). Plasma-Treated Water Affects Listeria Monocytogenes Vitality and Biofilm Structure. *Frontiers Microbiology, 12:652481. doi:10.3389/fmicb.2021.652481*

Plasma-treated water affects Listeria monocytogenes vitality and biofilm formation

Oliver Handorf (oliver.handorf@inp-greifswald.de)
Institute for plasma science and technology https://orcid.org/0000-0003-0786-5456
Viktoria Isabella Pauker
University of Greifswald, Institute of Microbiology
Thomas Weihe
Leibniz institute for plasma science and technology (INP)
Uta Schnabel
Leibniz institute for plasma science and technology (INP)
Eric Freund
Leibniz institute for plasma science and technology (INP), ZIK plasmatis
Sander Bekeschus
Leibniz institute for plasma science and technology (INP), ZIK plasmatis
Katharina Riedel
University of Greifswald, Institute of microbiology
Jörg Ehlbeck
Leibniz institute for plasma science and technology (INP)

Research article

Keywords: antimicrobial, atomic force microscopy, CFU, confocal laserscanning microscopy, fluorescence microscopy, food production industry, MidiPLexc, viability, XTT

DOI: https://doi.org/10.21203/rs.3.rs-31328/v1

Abstract

Plasma-generated compounds (PGCs) such as plasma-processed air (PPA) or plasma-treated water (PTW) offer an increasingly important alternative for the treatment of microorganisms in hard-to-reach areas found in several industrial applications including the food industry. To this end, we studied the antimicrobial capacity of plasma-treated water on the vitality and biofilm formation of *Listeria monocytogenes*, a common food spoilage microorganism. Using a microwave plasma (MidiPLexc), 10 ml of deionized water was treated for 100 s, 300 s and 900 s (pretreatment time) and the bacterial biofilm was subsequently exposed to the PTW for 1 min, 3 min and 5 min (posttreatment time) for each pretreatment time separately. Colony-forming units (CFU), metabolic activity, and cell vitality were reduced for 4.7 $\log_{10}$, 47.9%, and 69.5%, respectively. Live/dead staining and fluorescence microscopy showed a positive correlation between treatment and incubation times and reduction in vitality. Atomic force microscopy indicated a change in the plasticity of the bacteria. These results suggest a promising antimicrobial impact of plasma-treated water on *Listeria* monocytogenes, which may lead to more targeted applications of plasma decontamination in the food industry in the future.

1 Background

The application of plasma-generated compounds (PGC) such as plasma-treated water (PTW) and plasma-processed air (PPA) is an emerging field of research and development (1-3). Especially the food production industry reports frequent problems with contamination of food products or its processing facilities. Often the entry of microorganisms occurs via the food itself. Fruits or vegetables, but also meat and dairy products are exposed to a natural microbial load from their environment (4, 5). This problem has become increasingly important since the tremendous variety of ready-to-eat or ready-to-cook products in supermarkets (6). Another problem is that incorporated pathogens lead to colonization of the production facilities and to contamination of the washing water or other processing goods. Especially the disinfection of the washing water, with conventional methods but also with new plasma technologies, is of increasing importance for the industry in terms of environmental sustainability and thus cost-effectiveness (7-14).

This development shows that the trend is moving away from direct plasma treatment of products to the use of PGCs. In addition to the advantage that water is already used in the food industry anyway and could easily be replaced by PTW, PGCs also offer other advantages such as easy storage and transportation compared to direct plasma treatments (15).

As early as 1966, Gray et al. (16) published the first comprehensive review about *Listeria monocytogenes* and *Listeria* infections. Nowadays, the Gram-positive, rod-shaped bacterium is widely known for its food-borne infection pathways (17). For decades, several outbreaks of food-borne listeriosis were frequently reported in North America, Europe, and in a few Asian countries (18-20). *Listeria* is already introduced to slaughterhouses and other food processing plants, and because of its psychrophilic character, it is often found on refrigerated food products like meat, milk, and fish (21-25). The successful colonization of

food-processing plants by *L. monocytogenes* is enabled by its ability to adhere to all common surfaces occurring in food industry where it can form biofilms (26). After successful adhesion, biofilms continue to grow and form sufficient protection mechanisms against disinfection and mechanical cleaning, which are commonly used in the food-processing industry (27).

Recently, a growing number of studies on the pathogenicity mechanisms of *L. monocytogenes* have been published, which underlines its increasing importance in human and animal health care (28). *L. monocytogenes* is a facultative intracellular bacterium that can cause central nervous system (CNS) infections (29, 30). However, it has been shown that *L. monocytogenes* is ten times more effective in invading the CNS than common pathogens such as *Streptococcus pneumoniae* or Group B *Streptococci* (31).

Fever and gastroenteritis can be caused by *L. monocytogenes* (19, 32). There are a number of case studies, in which the pathogen was found on chocolate milk cartons, corn, and cold-smoked fish products (19, 33-35).

Besides CNS infection and febrile gastroenteritis, sepsis is one of the most common diseases caused by *L. monocytogenes* in immunosuppressed patients (36, 37). Less frequent are diseases like endocarditis, peritonitis, and focal infections (38). Therefore, *L. monocytogenes* is a highly pathogenic microorganism, and new efficient antimicrobial methods are urgently needed in the food industry to combat its impact as a food-borne pathogen.

2 Methods

2.1 Plasma source

The MidiPLexc (Fig. 1)(39) is a microwave-driven plasma source and an extension of the MiniMIP (40). In contrast to the MiniMIP, this plasma source can be operated with compressed air instead of argon gas, which leads to lower operation costs. In addition, it is possible to treat different amounts of liquids with the microwave-induced plasma gas, because of its integrated bottle adapter (39) (41). The MidiPLexc was operated with compressed air as working gas and a forward power of 80 W and a reverse power of 20 W. After 30 min running time to ensure a stable gas flow and effluent, the generation of plasma-treated water (PTW) was started.

2.2 Generation of the PTW by the MidiPLexc

A 1 l glass bottle was filled with 10 ml of deionized water (DW) and integrated into the bottle adapter of the MidiPLexc for the production of the PTW. In our experiments, we used the terms pre- and post-treatment times. The pre-treatment defines the contact time of the DW with the plasma gas and the post-treatment is equivalent to the contact time of the PTW with the biofilm. For the biological investigations, three different pre-treatment times (100 s, 300 s, 900 s) and three different post-treatment times (1 min, 3 min, 5 min) for each pretreatment time were used. Each post-treatment time for the biofilms was

performed in triplicates per experimental day. Each test was performed in four biological replicates. This yielded in n = 12 for each post-treatment time.

2.3 Bacterial strain and growth conditions

L. monocytogenes, (ATCC 15313) was used for cultivation because of its wellknown ability to form biofilms (42, 43). In the beginning, 1 l Brain Heart Infusion (BHI) broth (Roth, Karlsruhe, Germany) was prepared, autoclaved, and its pH value was adjusted to pH 6 by adding 10 M hydrochloric acid (HCl). This was adapted according to the results of a previous study (44). Additionally, the BHI medium was pumped through a 0.2 µm polyether sulfone (PES) filter system (VWR, Darmstadt, Germany) using a vacuum pump and was sterile filtrated. A colony was removed from an inoculated agar plate using a 10 µl inoculation loop, subsequently suspended in 50 ml BHI medium, and incubated for 24 h at 30 °C without shaking. On the next day, 1 ml of the suspension was diluted with BHI broth and adjusted to an optical density (OD) at 600 nm of 0.100 by using 10 mm diameter polystyrene cuvettes in a UV-3100PC Spectrophotometer (VWR, Darmstadt, Germany). This suspension was used for biofilm cultivation by pipetting 300 µl per well in a 96-well plate and incubated again for 24 h at 30 °C without shaking to ensure cell adhesion. Afterward, the medium was removed to discard the non-adhered cells, and 300 µl of fresh medium was added. After another 24 h of incubation at 30 °C in the dark without shaking, the PTW treatment was realized.

2.4 PTW treatment of L. monocytogenes biofilms

After careful removal of the medium, 300 µl PTW produced by the MidiPLexc for the different post-treatment times were added to the biofilms. Only one post-treatment time was performed at the same time to avoid any drying effects on the biofilms. Afterward, the PTW was removed, and the biofilm was mechanically detached from the surface, before being dissolved in 300 µl PBS (pH 7.2; according to Sörensen). To ensure the transfer of the entire biofilm, this step was repeated two times in total, which resulted in a final suspension volume of 600 µl. This suspension was used for Colony-forming units (CFU) assay (2.5), fluorescence assay (2.6), as well as XTT assay (2.7). The mechanical detachment of the biofilms was omitted for fluorescence microscopy (2.8), confocal laser scanningmicroscopy (CLSM) (0) and atomic force microscopy (AFM) (2.10).

2.5 Determination of the remaining CFU after PTW treatment

To determine the CFU after PTW treatment of the biofilm, 100 µl were taken from the 600 µl suspension (2.4), and a serial dilution was performed. This was done by diluting the specimen in a ratio of 1:10 with maximum recovery diluent (MRD; 0.85% NaCl, 1% tryptone). The controls were finally diluted 1:1,000,000 and the samples 1:1,000. Each dilution step was plated on BHI agar by pipetting 10 µl per dilution onto the plate and spread out by using the tilting technique. The plates were incubated for 24 h at 30 °C, without shaking. The colonies for the respective dilution levels were counted manually, and the CFU/ml values were calculated by using the formula: , where 10^x is the dilution factor for the lowest dilution, v is the volume of diluted cell suspension per plate in ml, $\sum c_y$ is the total number of colonies on all (n_y) plates

of the lowest evaluated dilution level, 10^{-x}, and $\sum c_{y+1}$ is the total number of colonies on all (n_{y+1}) plates of the next-highest dilution level evaluated, $10^{-(x+1)}$. The calculation is explained in more detail in (45).

The propagation of error was calculated for each treatment group. This finally resulted in 4 different error propagations for each treatment time, from which the weighted error was calculated and used as error bars in the illustration (Fig. 2) (46). The experiments were repeated fourfold with n = 3, which finally resulted in n = 12.

2.6 Fluorescence LIVE/DEAD assay

The LIVE/DEAD BacLight Bacterial Kit (Thermo Scientific, Waltham, USA) was prepared according to product instructions. Finally, 0.9 µl of the mixture were added to 300 µl of the specimen, followed by incubation on a rotary shaker at 30 rpm in the dark at room temperature for 20 min. A fluorescence microplate-reader (Varioskan-Flash®, Thermo Scientific, Waltham, USA) was used to determine the fluorescence of each well of the 96-well plate with an excitation wavelength of 470 nm and an emission wavelength of 530 nm or 630 nm for green (G) and red (R) fluorescence. Conclusively, a ratio G/R was calculated by dividing the intensity value of red fluorescence by the value of green fluorescence. The ratio G/R values of the controls and samples were expressed as a percentage in relation to each other and were graphically displayed using Origin 2019b software (OriginLab, Northhampton, USA). The experiments were repeated fourfold with n = 3, which finally resulted in n = 12.

2.7 XTT assay

A colorimetric assay was used to determine the cell vitality after plasma treatment (XTT Cell Proliferation Assay Kit, Applichem, St. Louis, USA). Therefore, the XTT assay revealed the cell vitality as a function of redox potential, which arises from a trans-plasma membrane electron transport (47). N-methyl dibenzopyrazine methylsulfate (PMS) was used as an intermediate electron carrier, which serves as an activator of the intended reaction. The XTT solution were mixed 1:50 with the activator solution and pipetted 1:3 to the samples, afterward. The 96well plate was incubated at 37 °C with continuous horizontal shaking (80 rpm) in the dark for 20–24 h. After the incubation time, the 96-well plate was scanned at a wavelength of 470 nm using the Varioskan-Flash® device. The obtained values were blank-corrected using XTT and the activation solution mix without bacterial suspension and scanned at a wavelength of 670 nm. The experiments were repeated fourfold with n = 3, which finally resulted in n = 12. The absorption values of the controls and samples were expressed as a percentage in relation to each other and were graphically displayed using Origin 2019b software.

2.8 Fluorescence microscopy

For fluorescence microscopy, transparent 96-well plates (Eppendorf, Hamburg, Germany) were used to grow biofilms. The LIVE/DEAD BacLight Kit (containing SYTO9 to stain all microorganisms, and propidium iodide (PI) to stain dead cells) was used according to the manufacturer's protocol. Widefield fluorescence images were acquired using an Operetta CLS high content imaging device (PerkinElmer,

Hamburg, Germany). For wholewell imaging, four fields of view were stitched digitally. A 5x objective (air, NA = 0.16, Zeiss, Oberkochen, Germany) was used. SYTO9 was excited by a 475 nm (110 mW) LED, and the fluorescence was collected with a 525 ± 25 nm bandpass filter. PI was excited by a 550 nm (170 mW) LED, and the emission light was collected with a 610 ± 40 nm bandpass filter. Laser autofocus (785 nm) provided exact focusing across all fields of view. For display, three stacks were merged into a maximum intensity projection to account for topographical particularities in the z-plane (focus ± 25 µm). For 3D images of biofilms, 30 z-planes (stacks) with 1.5 µm between each plane were measured using a 40x air objective (NA = 0.6). Three-dimensional reconstruction, image stitching, and quantification were done using Harmony 4.8 software (PerkinElmer, Hamburg, Germany).

2.9 CLSM

Biofilms were cultivated, plasma-treated, and LIVE/DEAD™ stained as described above (2.8). After the staining, the supernatants were removed and the biofilms were analyzed using a Zeiss LSM 510 microscope (Carl Zeiss, Jena, Germany) equipped with a 63 × objective (water, NA = 0.1). Filter and detector settings for monitoring SYTO9 and PI fluorescence (excitation at 488 nm using an argon laser, emission light of SYTO9 selected with a 505–530 nm band pass filter, emission light of PI selected with a 650 nm long pass filter). Three-dimensional images were acquired using the ZEN 2009 software (Carl Zeiss, Jena, Germany) with an area of 100 µm × 100 µm and z-stack sections of 5 µm.

2.10 Atomic-force microscopy

Since the AFM can only measure smaller samples in the measurement holder, an alternative to the 96-well plates had to be found. For this purpose, the biofilms for AFM measurements were grown on sterile polyethylene terephthalate, glycol-modified (PET-G) cover slips (13 mm, Sarstedt, Nümbrecht, Germany). For better adhesion of the coverslips to the bottom of the well plates and to avoid growth of the bacteria at the reverse side of the coverslips, 50 ml Gelrite (Duchefa, Haarlem, Netherlands) was autoclaved and directly used after the autoclaving process due to a rapid thermal curing process. A volume of 1 ml liquid Gelrite were pipetted to each well of a 12-well plate. The coverslips were placed at the surface of the liquid Gelrite and were thermally cured. The biofilms were cultivated as described above and 1 ml of BHI broth was pipetted to each well until the coverslips were topped with the medium. 12-well plates were incubated at 30 °C for 24 h without shaking. After the incubation time, the consumed BHI broth was removed to take non-adhered cells away. Subsequently, 1 ml fresh BHI broth was added to the wells, followed by an additional incubation at 30 °C for 24 h. The next day, the cultivation medium was removed and the coverslips with biofilms were treated for 5 min with the different PTWs of 100 s, 300 s and 900 s pre-treatment time. Dehydration of the coverslips before AFM analysis was avoided by using a humidity chamber. The AFM measurements were carried out on a DI CP II SPM (Veeco, Plainview, USA), which was mounted on a vibration-free object table (TS150, TableStable, Zwillikon, Switzerland). The setup was standing on an optical bench encased by an additional acoustic protection. The AFM was equipped with a linearized piezo scanner, on which the coverslips were mounted on a metal sample holder with leading tabs. The samples were measured using cantilevers (PLANO GmbH, Wetzlar, Germany) with nominal

spring constants of k = 0.1–0.6 N/m in contact mode. The pictures were taken by a scanning speed of 0.4 Hz by a picture size of 20 μm^2 and a set point = 8 N/m. Pictures were edited with Gwyddion (Czech Metrology Institute, Brno, Czech Republic).

3 Results

3.1 Optimal treatment window of pre-treatment and post-treatment times concerning the reduced proliferation of biofilm cells.

The cell proliferation assay showed a reduction of 1.95×10^8 cells (RF of 1.71) already after 100 s pre-treatment time. This is on the rise with increasing post-treatment times (RF of 2.66 after 5 min). With a longer pre-treatment time, even a stronger reduction of 2.66×10^8 cells could be observed, which corresponds to an RF of 3.84 (300 s, 3 min) and 2.94×10^7, which corresponds to an RF of 3.73 (900 s, 3 min) (Fig. 2). With a pre-treatment time of 300 s and longer, the highest reductions were achieved with a post-treatment time of 3 min and slightly lower reductions were achieved with longer post-treatment times (5 min) (Fig. 2). In terms of total cell counts, the strongest influence on cell proliferation was measured after 300 s, 3 min PTW treatment. In total, a maximum reduction of *L. monocytogenes* biofilm cells from 2.67×10^8 to 4.68×10^8 was achieved.

3.2 PTW treatment leads to a strong reduction in the vitality of biofilm cells

The results of the vitality assay at a pre-treatment time of 100 s showed that a significant reduction of vitality of up to 25.9 % could only be achieved after 5 min post-treatment time (Fig. 3). With a pre-treatment time of 300 s, a reduction of up to 45.8 % could be achieved after 1 min post-treatment time. This increased progressively to 58.1 % (300 s, 3 min), and 64.5 % (300 s, 5 min) (Fig. 3, center). The increasing reduction could also be measured at 900 s pre-treatment time. In this case, the strongest measured reduction in vitality of up to 69.5 % occurs after 5 min post-treatment time (Fig. 3, right).

3.3 The reduction of the metabolism of biofilm cells was only detectable after long pre-treatment and post-treatment times

By measuring the reduction of the metabolic activity of the biofilm cells after PTW treatment, no significant change could be observed at 100 s pre-treatment time despite the length of the post-treatment time (Fig. 4, left). If PTW was used, which was treated with the MidiPLexc for 300 s, only very low reductions with a maximum of 9.1 % (300 s, 5 min) could be detected in the various post-treatment times

(Fig. 4, center). At 900 s pre-treatment time, comparable reductions of 11.4 % (900 s, 3 min) could be detected. However, a significantly higher reduction of 47.95 % could be demonstrated at 900 s pre-treatment and 5 min post-treatment time, where the dynamic effect of the metabolism of the cells begins (Fig. 4, right).

3.4 The antimicrobial characteristics of substances frequently used in the food industry are partially pH value specific

The treatment of DW for 900 s led to a pH value of the solution of 1.27. To investigate whether the antimicrobial effect of PTW compared to 0.3 % (3 g/l) chlorine dioxide (ClO_2) was based on the different pH values of these solutions, the antimicrobial effect of the substances in their original pH value was compared with the antimicrobial effect of the pH value adapted to the pH of the PTW with respect to CFU (Fig. 5), fluorescence (Fig. 6) and XTT assay (Fig. 7). The CFU count showed a strong pH dependence for ClO_2 and a slight dependence for 10 M HCl (Fig. 5). These effects were confirmed in the fluorescence assay. Here, a strong pH dependence could also be observed for ClO_2 (Fig. 6). However, a strong dependence for 10 M HCl also becomes apparent in this case. Interestingly, the effect on cell metabolism for all substances is extremely pH dependent. In this case, a clear effect could also be observed with 70 % alcohol (Fig. 7). ClO_2 in its used concentration, which is a very high concentration for sanitizing the wash water of food products, has a pH value of 4.288, which means that the pH value was lowered by 3.017 in the experiment. This showed that ClO_2 only unfolds its antimicrobial effect in very low pH ranges. Nevertheless, the antimicrobial effect of ClO_2 could exceed that of PTW only in the XTT assay even at low pH ranges (Fig. 7). Here a reduction of the metabolism of 89 % was achieved compared to 33 % for PTW. With 10 M HCl, the effect was antagonistic. Here the pH value of the 10 M HCl, which was -1.609 in the used concentration, was increased by a pH value of 2.88. This has only a slightly weaker effect on the proliferation of the cells with 10 M HCl, but a very strongly weakened effect on the vitality and metabolism of the cells.

3.5 Fluorescence microscopy revealed inactivation kinetics from the top to the bottom of the biofilm

All fluorescence microscopic images are inverse footages of the biofilms. The cells of the untreated biofilm showed only vital (green fluorescence) cells (Fig. 8A). The 3D images of the same footage confirmed this and showed a very dense biofilm with mushroom-shaped ridges within the biofilm extending to a height of about 60 µm whereas the average biofilm was limited to a thickness of about 20 µm. This area is characterized by a strong staining, which resulted in a very dense structure compared to the mushroom-shaped areas. (Suppl. Fig 1). The treated biofilms showed progressively more inactivated cells with increasing treatment time up to 900 s treatment time (Figs. 8B-J). The 3D image of the 900 s

pre-treated biofilm showed a nearly completely dead biofilm (Suppl. Fig. 2). Only a few very small hotspots of living cells were visible in the biofilm. The dynamics comparing the different treatment times showed that the inactivation started in the center and expanded to the outside (Figs. 8B-E).

3.6 CLSM showed a partial inactivation of biofilms predominantly in the central area

The control biofilms showed continuous living cells and a relaxed structure (Fig. 9, topographical view). After 100 s pre-, 5 min post-treatment there was no change in the live/dead staining of the biofilm cells. Only living cells were visible in the biofilm, but they appeared much denser compared to the control biofilm (Fig. 9, see 100 s pre-, 5 min post-treatment). After 300 s pre-, 5 min post-treatment time no changes in the thickness of the biofilms compared to the control biofilm could be detected. The biofilms were about 10 µm thick as well as the control biofilms. However, mainly cells in the central area of the biofilm were stained yellow, which indicates inactivation of the cells but no death (Fig. 9, see 300 s pre-, 5 min post-treatment). After 900 s pre- 5 min post-treatment, there was no change in the staining of the cells compared to the 300 s treatment. However, there was a significant removal of biofilm mass of about 6 µm, resulting in a biofilm thickness of 4 µm (Fig. 9, see 900 s pre-, 5 min post-treatment). The biofilm matrix appeared absolutely flat with a homogenous structure.

3.7 AFM images showed alterations in the plasticity of the biofilm surface

The AFM images of the control biofilms showed long blurred lines of the biofilm surface, which allowed conclusions about the softness of the surface (Fig. 10A). In contrast, the treated biofilms could be displayed very well defined and structured (Fig. 10B). Concerning the cell morphology, there was hardly any change visible after treatment. However, comparison cells of biofilms that came into contact with 100 s pre-treated PTW to 300 s and 900 s pre-treated PTW, appeared significantly larger and somehow swollen (Figs. 10B-D).

4 Discussion

monocytogenes is feared as a dangerous pathogen in food-production industry. Interestingly, *L. monocytogenes* contaminations, especially of meat and dairy products, ranked only 8th among the most common disease outbreaks in the USA, following pathogens such as *Salmonella*, *Clostridium perfringens*, *Campylobacter*, *Escherichia coli*, *Bacillus cereus*, *Staphylococcus aureus* and *Vibrio parahaemolyticus (48)*. However, the extent of *Listeria* infections is devastating. Statistics showed that every infection with *L. monocytogenes* lead to hospitalization (48, 49). If immunocompromised patients were affected, *L. monocytogenes* infections were often lethal. Today´s society, where the incidence of food-borne diseases are no longer as high as it was the case a few decades ago, there is an increasing focus on serious

infections caused by food contaminants that do not occur regularly. Conventional methods of food decontamination for fresh food include peracitic acid, lactic acid, chlorination and treatment with diluted chlorine dioxide or ozone. Chlorination of food is already banned in most European Union (EU) countries due to human health hazards, but is still used in The United States or Brazil (50-53). The use of diluted chlorine dioxide is permitted in the EU under well-defined regulations in the industry. Due to the risk of infection from fresh food, new innovative methods are increasingly being researched, which are more efficient and less problematic than previous methods, but at the same time simple and cost-effective in its use and do not cause significant alterations to the product itself (54). Since the efficiency of the washing and sanitation processes are directly related to the microbiological quality of the end-product, companies are interested in the continuous optimization of these processes (55, 56). Investigations showed that plasma or PGCs do not cause any changes in the texture and color of the food and still cause a significant reduction in the bacterial contamination (57-59). Due to the fact that many plasma sources nowadays can be operated with ambient air and tap water as a treatment source for food, the process is cost efficient and ecological. The MidiPLexc used in this work fulfills these requirements for a plasma source and could be used for industrial purposes by upscaling.

Nevertheless, the detailed mechanisms of the PGC effects remain unclear, but recent studies revealed a coherence of the antimicrobial potential with the concentration of reactive oxygen (ROS) and nitrogen (RNS) species (39, 41).

In the presented study, the microwave-induced MidiPLexc plasma source provides a temperature regime that favors the production of RNS such as nitrate (NO_3^-), nitrite (NO_2^-), and nitrogen monoxide (NO). Beside these dominating compounds, peroxynitrite ($ONOO^-$) and hydrogen peroxide (H_2O_2) has been generated in various quantities and may be considered as intermediates for more stable RNS or ROS, respectively (39).

Generally, acidification of the PTW adds to its antimicrobial effect (60), by contributing to chemical redox reactions within the PTW (61). For instance, the reaction of $ONOO^-$ to the peroxonitric acid (HNO_4) seems to be a pivotal factor. This is, followed by the reactions of nitrous acid (HNO_2) and nitric acid (HNO_3), which derive from NO_2^- and NO_3^-, respectively, and seem to be responsible for the antimicrobial effect of PTW.

An influence of the temperature can be excluded (39). Even direct biofilm treatments with the MiniMIP, the previous version of the MidiPLexc, revealed no temperature influences on the antimicrobial behavior against biofilms (45). Additionally, the temperature increases by approx. 3.5 °C only during the production of PTW with the MidiPLexc (39). Consequently, the antimicrobial effect of a PTW solution is achieved by the reactive oxygen/nitrogen species (RONS).

The investigation of the effects of PTW in the field of decontamination of food and surfaces in food production is still in its infants. While there have been numerous studies investigating the effects of plasma gas on food products (1, 62-65), surfaces (66-68) and packaging (69, 70), less has been reported

about the treatment with PTW (59, 71-73). The treatment of *L. monocytogenes* monospecies and multispecies biofilms with *Pseudomonas fluorescens* on lettuce with plasma gas resulted in reductions to undetectable levels after 60 s treatment time for the monospecies biofilms and a reduction of 2.2 $\log_{10}$ steps for *L. monocytogenes* in a multispecies biofilm with *P. fluorescens* (74). It has been shown that multispecies biofilms of *L. monocytogenes* showed a higher resistance against plasma gas than monospecies biofilms. In our work, we demonstrated that *L. monocytogenes* biofilms have a much higher resistance against PGCs than other bacteria like *P. fluorescens* (41).

In the field of antimicrobial research of plasma and PGCs, the effect of these substances on the extracellular polymeric substances (EPS) of biofilms becoming increasingly important. However, the effect of PTW on different EPS is still not fully understood. Thus, a comparison with other studies is very difficult, since in addition to the plasma source and application method (PPA or PTW), the pathogen strain (75), growth time and treatment time also play an important role. In addition, the growth temperature (74) and the overgrown material or food product (76) also have a decisive influence. A previous conducted and comparable study to this work showed the effect of PTW on *P. fluorescens* monospecies biofilms. It demonstrated a reduction of 6 $\log_{10}$ steps compared to a control biofilm with a CFU of 10 $\log_{10}$. Mechanistically, a clear removal of the biofilm material by the PTW treatment could be proven as well as cell death within that work (41). In the present study, a reduction of about 5 $\log_{10}$ steps compared to a control biofilm of 8 $\log_{10}$ was detectable. The important difference compared with the previous study, however, lies in the vitality and metabolism results and in the microscopic analysis. For the *L. monocytogenes* biofilms, a removal of the biofilm material could also be proven, but a significantly lower effect in the LIVE/DEAD assay in combination with the 3D image of the CLSM **(suppl. Material)**. On the one hand, this again showed the compelling evidence of further investigations concerning the effects of PTW besides the CFU assay and, on the other hand, it rather indicates an inactivation of the cells more than cell death.

The effect of plasma on the extracellular matrix can be decisive. Various studies have already demonstrated the effect of plasma on the EPS of biofilms (77-80). Studies have shown that different species can produce various amounts of EPS (32, 81). Furthermore, the composition of the different EPS of the pathogens could also play an important role. *P. fluorescens* generates EPS matrix, which is rich in proteins and carbohydrates. The dominant components are proteins, which may explain the mucous nature of the biofilms in combination with polysaccharides (32, 82, 83). *L. monocytogenes,* strain ATCC 15313 forms a thick and compact matrix, which seems to contain much less EPS, which mainly covers the overgrown surface. The EPS of *L. monocytogenes* consists of mainly polysaccharides and teichoic acids (84). This results in differences in the physical composition of the biofilm and its properties and therefore, could explain their higher resistance to plasma treatment shown in this work.

This raises the question about the effect of EPS on plasma treatments. It is well established that EPS has a protective effect for the biofilm during plasma treatment with plasma gas or direct contact with the plasma effluent. However, the results of this work in combination with our previous work showed a rather

antagonistic effect (41). This could be due to the high water binding capacity of the biofilm (85-87). Macroscopically, when treating the biofilms with PTW, it is easy to see that the PTW is partly completely absorbed by the biofilm. This absorption leads to a certain dilution effect of the concentrated components of the PTW, but also to a longer contact time with the cells of the biofilm beyond the actual post-treatment time. With the high concentrations of nitrite and nitrate, as used after the pre-treatment times applied for *L. monocytogenes* biofilm treatment, the dilution effects of the EPS play a rather minor role (39). With regard to the application, a further concentration of the water contained in the EPS by subsequent plasma gas treatment could have a far-reaching synergistic effect. This effect has already been demonstrated in previous work and will most likely be further enhanced by the enrichment of the PTW components in the biofilm matrix (15).

Summarizing, this work shows the complexity of the problem of microbiological contamination in the food production industry. Different pathogens and applications require different experimental setups. Therefore, the choice of plasma source, settings and treatment times must always be adapted to the fundamental problem in the industry. The pre-treatment time of the PTW seems to be more decisive for the antimicrobial effect than the post-treatment time on the *L.* monocytogenes biofilm. Thus, this work forms a basis to establish a universal application plan for the requirements in the food industry to be able to meet their demands in the future.

Conclusion

This work vividly demonstrates the complexity of the effect of PGCs on *L. monocytogenes* biofilms. The complex implementation of microbiological methods and their interpretation as a sophisticated system clearly showed that these investigations can only be evaluated as an all-embracing system. While single results like the CFU showed considerable reductions, the microscopic images show rather minor membrane damages of the cells. In comparison to already published studies, this work shows that a decisive factor in the antimicrobial effect of PTW is the cell membrane structure of the bacteria and that Gram-positive pathogens such as *L. monocytogenes* seems to be much more resistant to PTW treatment than Gram-negative pathogens like *P. fluorescens*. This is of crucial importance for industrial applications.

5 Abbreviations

AFM atomic force microscopy

BHI Brain Heart Infusion

CFU colony forming units

ClO_2 chlorine dioxide

CLSM confocal laser scanning microscopy

CNS central nervous system

DW deionized water

EPS extracellular polymeric substances

EU European Union

HCl hydrochloric acid

MRD maximum recovery diluent

NO nitrogen monoxide

NO_2^- nitrite

NO_3^- nitrate

OD optical density

PET-G polyethylene terephthalate, glycol - modified

PES polyether sulfone

PGC plasma-generated compound

PI Propidium Iodide

PMS N-methyl dibenzopyrazine methylsulfate

PPA plasma-processed air

PTW plasma-treated water

RF reduction factor

RNS reactive nitrogen species

ROS reactive oxygen species

Declarations

6.1 Author contribution

O.H: Writing the publication, performing the CFU, fluorescence and XTT assays, accompanying the CLSM and AFM experiments. Incorporation of the corrections. Image editing and data processing.

V.I.P: Performance of the CLSM experiments. Correction of the manuscript. Generation and editing of the CLSM images.

T.W: Performance of the AFM experiments. Correction of the manuscript. Generation and editing of the AFM images.

U.S: Mentoring of the project. Correction of the manuscript.

E.F: Performance of the fluorescence microscopy. Correction of the manuscript. Generation and editing of the fluorescence microscopy images.

S.B: Performance of the fluorescence microscopy. Correction of the manuscript. Generation and editing of the fluorescence microscopy images. Acquisition of the funding for the fluorescence microscopy experiments.

K.R: Mentoring of the project and the PhD thesis of O.H. which includes this manuscript. Correction of the manuscript. Acquisition of the funding for the project.

J.E: Mentoring of the project and the PhD thesis of O.H. which includes this manuscript. Correction of the manuscript.

6.2 Ethics approval and consent to participate

Not applicable

6.3 Consent for publication

Not applicable

6.4 Availability of data and materials

The datasets used and/or analysed during the current study are available from the corresponding author on reasonable request.

6.5 Competing interests

The authors declare that they have no competing interests.

6.6 Funding

This research was funded by the DFG “German Research Association”, grant number CRC TRR34, subproject A3 (Katharina Riedel, Viktoria Isabella Pauker). This research was also funded by the BMBF “German Federal Ministry of Education and Research”, grant number 03Z22DN11 (Sander Bekeschus, Eric Freund). The funding was provided in the form of project-related funds for the acquisition of materials and jobs. The funding agencies had no influence on the results of this study.

6.7 Acknowledgements

We would like to thank Dr. Katja Fricke for the provision of the AFM. We would also like to thank the Imaging Center of the Department of Biology, University of Greifswald for the provision of the CLSM.

References

1. Schnabel U, Schmidt C, Stachowiak J, Bosel A, Andrasch M, Ehlbeck J. Plasma processed air for biological decontamination of PET and fresh plant tissue. Plasma Process Polym. 2018;15(2).
2. Andrasch M, Stachowiak J, Schluter O, Schnabel U, Ehlbeck J. Scale-up to pilot plant dimensions of plasma processed water generation for fresh-cut lettuce treatment. Food Packaging Shelf. 2017;14:40-5.
3. Schnabel U, Andrasch M, Stachowiak J, Weit C, Weihe T, Schmidt C, et al. Sanitation of fresh-cut endive lettuce by plasma processed tap water (PPtW) – Up-scaling to industrial level. Innov Food Sci Emerg. 2019;53:45-55.
4. Heyndrickx M. The Importance of Endospore-Forming Bacteria Originating from Soil for Contamination of Industrial Food Processing. Applied and Environmental Soil Science. 2011;2011(Microbial Diversity-Sustaining Earth and Industry):11.
5. Matthews KR, Sapers GM, Gerba CP. The Produce Contamination Problem. Food Science and Technology. 2014;2:492.
6. Rodgers S. Long shelf life cook-chill technologies: food safety risks and solutions. Food Aust. 2003;55(3):80-3.
7. Banach JL, Sampers I, Van Haute S, van der Fels-Klerx HJ. Effect of Disinfectants on Preventing the Cross-Contamination of Pathogens in Fresh Produce Washing Water. Int J Env Res Pub He. 2015;12(8):8658-77.
8. Gil MI, Selma MV, Lopez-Galvez F, Allende A. Fresh-cut product sanitation and wash water disinfection: Problems and solutions. Int J Food Microbiol. 2009;134(1-2):37-45.
9. Selma MV, Allende A, Lopez-Galvez F, Conesa MA, Gil MI. Disinfection potential of ozone, ultraviolet-C and their combination in wash water for the fresh-cut vegetable industry. Food Microbiol. 2008;25(6):809-14.
10. Van Haute S, Sampers I, Holvoet K, Uyttendaele M. Physicochemical Quality and Chemical Safety of Chlorine as a Reconditioning Agent and Wash Water Disinfectant for Fresh-Cut Lettuce Washing.

Appl Environ Microb. 2013;79(9):2850-61.

11. Gil MI, Gomez-Lopez VM, Hung YC, Allende A. Potential of Electrolyzed Water as an Alternative Disinfectant Agent in the Fresh-Cut Industry. Food Bioprocess Tech. 2015;8(6):1336-48.
12. Rowan NJ, Espie S, Harrower J, Anderson JG, Marsili L, MacGregor SJ. Pulsed-plasma gas-discharge inactivation of microbial pathogens in chilled poultry wash water. J Food Protect. 2007;70(12):2805-10.
13. Cullen PJ, Lalor J, Scally L, Boehm D, Milosavljevic V, Bourke P, et al. Translation of plasma technology from the lab to the food industry. Plasma Process Polym. 2018;15(2).
14. Patange A, Lu P, Boehm D, Cullen PJ, Bourke P. Efficacy of cold plasma functionalised water for improving microbiological safety of fresh produce and wash water recycling. Food Microbiol. 2019;84.
15. Schnabel U, Handorf O, Yarova K, Zessin B, Zechlin S, Sydow D, et al. Plasma-Treated Air and Water-Assessment of Synergistic Antimicrobial Effects for Sanitation of Food Processing Surfaces and Environment. Foods. 2019;8(2).
16. Gray ML, Killinger AH. Listeria Monocytogenes and Listeric Infections. Bacteriol Rev. 1966;30(2):309-+.
17. Farber JM, Peterkin PI. Listeria-Monocytogenes, a Food-Borne Pathogen. Microbiol Rev. 1991;55(3):476-511.
18. Wehr HM. Listeria-Monocytogenes - a Current Dilemma. J Assoc Off Ana Chem. 1987;70(5):769-72.
19. Dalton CB, Austin CC, Sobel J, Hayes PS, Bibb WF, Graves LM, et al. An outbreak of gastroenteritis and fever due to Listeria monocytogenes in milk. New Engl J Med. 1997;336(2):100-5.
20. Makino SI, Kawamoto K, Takeshi K, Okada Y, Yamasaki A, Yamamoto S, et al. An outbreak of food-borne listeriosis due to cheese in Japan, during 2001. Int J Food Microbiol. 2005;104(2):189-96.
21. Schlech WF. Expanding the Horizons of Foodborne Listeriosis. Jama-J Am Med Assoc. 1992;267(15):2081-2.
22. Wilkins PO, Bourgeois R, Murray RG. Psychrotrophic properties of Listeria monocytogenes. Can J Microbiol. 1972;18(5):543-51.
23. Glass KA, Doyle MP. Fate of Listeria-Monocytogenes in Processed Meat-Products during Refrigerated Storage. Appl Environ Microb. 1989;55(6):1565-9.
24. Farber JM. Listeria-Monocytogenes in Fish Products. J Food Protect. 1991;54(12):922-4.
25. Hayes PS, Feeley JC, Graves LM, Ajello GW, Fleming DW. Isolation of Listeria-Monocytogenes from Raw-Milk. Appl Environ Microb. 1986;51(2):438-40.
26. Møretrø T, Langsrud S. Listeria monocytogenes: biofilm formation and persistence in food-processing environments. Cambridge University Press. 2004;1(2):107-21.
27. Blackman IC, Frank JF. Growth of Listeria monocytogenes as a biofilm on various food-processing surfaces. J Food Protect. 1996;59(8):827-31.

28. Cossart P, Mengaud J. Listeria-Monocytogenes - a Model System for the Molecular Study of Intracellular Parasitism. Mol Biol Med. 1989;6(5):463-74.
29. Vazquez-Boland JA, Kuhn M, Berche P, Chakraborty T, Dominguez-Bernal G, Goebel W, et al. Listeria pathogenesis and molecular virulence determinants. Clin Microbiol Rev. 2001;14(3):584-+.
30. Drevets DA, Bronze MS. Listeria monocytogenes: epidemiology, human disease, and mechanisms of brain invasion. Fems Immunol Med Mic. 2008;53(2):151-65.
31. Schuchat A, Robinson K, Wenger JD, Harrison LH, Farley M, Reingold AL, et al. Bacterial meningitis in the United States in 1995. New Engl J Med. 1997;337(14):970-6.
32. O'Toole G, Kaplan HB, Kolter R. Biofilm formation as microbial development. Annu Rev Microbiol. 2000;54:49-79.
33. Aureli P, Fiorucci GC, Caroli D, Marchiaro G, Novara O, Leone L, et al. An outbreak of febrile gastroenteritis associated with corn contaminated by Listeria monocytogenes. New Engl J Med. 2000;342(17):1236-41.
34. Miettinen MK, Siitonen A, Heiskanen P, Haajanen H, Bjorkroth KJ, Korkeala HJ. Molecular epidemiology of an outbreak of febrile gastroenteritis caused by Listeria monocytogenes in cold-smoked rainbow trout. J Clin Microbiol. 1999;37(7):2358-60.
35. Ooi ST, Lorber B. Gastroenteritis due to Listeria monocytogenes. Clin Infect Dis. 2005;40(9):1327-32.
36. Lorber B. Listeriosis. Clin Infect Dis. 1997;24(1):1-11.
37. Büla CJ, Bille J, Glauser MP. An Epidemic of Food-Borne Listeriosis in Western Switzerland - Description of 57 Cases Involving Adults. Clin Infect Dis. 1995;20(1):66-72.
38. Doganay M. Listeriosis: clinical presentation. Fems Immunol Med Mic. 2003;35(3):173-5.
39. Handorf O, Below H, Schnabel U, Riedel K, Ehlbeck J. Investigation of the chemical composition of plasma treated water by MidiPLexc and its antimicrobial effect on Listeria monocytogenes and Pseudomonas fluorescens monospecies suspension cultures. Journal of Physics D: Applied Physics. 2020.
40. Baeva M, Bösel A, Ehlbeck J, Loffhagen D. Modeling of microwave-induced plasma in argon at atmospheric pressure. Phys Rev E. 2012;85(5).
41. Handorf O, Pauker VI, Schnabel U, Weihe T, Freund E, Bekeschus S, et al. Characterization of Antimicrobial Effects of Plasma-Treated Water (PTW) Produced by Microwave-Induced Plasma (MidiPLexc) on Pseudomonas fluorescens Biofilms MDPI - Applied Sciences. 2020;10(9: Special Issue: Application of Plasma Technology in Bioscience and Biomedicine):3118.
42. Borges A, Saavedra MJ, Simoes M. The activity of ferulic and gallic acids in biofilm prevention and control of pathogenic bacteria. Biofouling. 2012;28(7):755-67.
43. Vazquez-Sanchez D, Galvao JA, Oetterer M. Contamination sources, serogroups, biofilm-forming ability and biocide resistance of Listeria monocytogenes persistent in tilapia-processing facilities. J Food Sci Tech Mys. 2017;54(12):3867-79.

44. Buchanan RL, Bagi LK. Microbial competition: effect of Pseudomonas fluorescens on the growth of Listeria monocytogenes. Food Microbiol. 1999;16(5):523-9.
45. Handorf O, Schnabel U, Bsel A, Weihe T, Bekeschus S, Graf AC, et al. Antimicrobial effects of microwave-induced plasma torch (MiniMIP) treatment on Candida albicans biofilms. Microb Biotechnol. 2019;12(5):1034-48.
46. Gränicher WHH. Messung beendet - was nun? Hochschulverlag AG der ETH Zürich. 1994:6-4 - 6-9.
47. Scudiero DA, Shoemaker RH, Paull KD, Monks A, Tierney S, Nofziger TH, et al. Evaluation of a Soluble Tetrazolium Formazan Assay for Cell-Growth and Drug Sensitivity in Culture Using Human and Other Tumor-Cell Lines. Cancer Research. 1988;48(17):4827-33.
48. CDC. Surveillance for Foodborne Disease Outbreaks United States, 2017: Annual Report. Center for Disease Control and Prevention - Annual Report. 2017:1-15.
49. RKI. Infektionsepidemiologisches Jahrbuch meldepflichtiger Krankheiten für 2018. Robert Koch institue - Annual Report. 2018:247.
50. Rico D, Martin-Diana AB, Barat JM, Barry-Ryan C. Extending and measuring the quality of fresh-cut fruit and vegetables: a review. Trends Food Sci Tech. 2007;18(7):373-86.
51. Jose JFBS, Vanetti MCD. Effect of ultrasound and commercial sanitizers in removing natural contaminants and Salmonella enterica Typhimurium on cherry tomatoes. Food Control. 2012;24(1-2):95-9.
52. Nguyenthe C, Carlin F. The Microbiology of Minimally Processed Fresh Fruits and Vegetables. Crit Rev Food Sci. 1994;34(4):371-401.
53. Baur S, Klaiber R, Hammes WP, Carle R. Sensory and microbiological quality of shredded, packaged iceberg lettuce as affected by pre-washing procedures with chlorinated and ozonated water. Innovative Food Science & Emerging Technologies. 2004;5(1):45-55.
54. Misra NN, Tiwari BK, Raghavarao KSMS, Cullen PJ. Nonthermal Plasma Inactivation of Food-Borne Pathogens. Food Eng Rev. 2011;3(3-4):159-70.
55. Ramos B, Miller FA, Brandao TRS, Teixeira P, Silva CLM. Fresh fruits and vegetables-An overview on applied methodologies to improve its quality and safety. Innovative Food Science & Emerging Technologies. 2013;20:1-15.
56. do Rosario DKA, Mutz YD, Peixoto JMC, Oliveira SBS, de Carvalho RV, Carneiro JCS, et al. Ultrasound improves chemical reduction of natural contaminant microbiota and Salmonella enterica subsp enterica on strawberries. Int J Food Microbiol. 2017;241:23-9.
57. Vleugels M, Shama G, Deng XT, Greenacre E, Brocklehurst T, Kong MG. Atmospheric plasma inactivation of biofilm-forming bacteria for food safety control. Ieee Transactions on Plasma Science. 2005;33(2):824-8.
58. Go SM, Park MR, Kim HS, Choi WS, Jeong RD. Antifungal effect of non-thermal atmospheric plasma and its application for control of postharvest Fusarium oxysporum decay of paprika. Food Control. 2019;98:245-52.

59. Xu YY, Tian Y, Ma RN, Liu QH, Zhang J. Effect of plasma activated water on the postharvest quality of button mushrooms, Agaricus bisporus. Food Chem. 2016;197:436-44.
60. Oehmigen K, Hähnel M, Brandenburg R, Wilke C, Weltmann KD, von Woedtke T. The Role of Acidification for Antimicrobial Activity of Atmospheric Pressure Plasma in Liquids. Plasma Processes and Polymers. 2010;7(3-4):250-7.
61. Ikawa S, Kitano K, Hamaguchi S. Effects of pH on Bacterial Inactivation in Aqueous Solutions due to Low-Temperature Atmospheric Pressure Plasma Application. Plasma Process Polym. 2010;7(1):33-42.
62. Schnabel U, Andrasch M, Niquet R, Weltmann KD, Schlüter O, Ehlbeck J. Non-Thermal Atmospheric Pressure Plasmas for Food Decontamination. International Proceedings of Chemical, Biological and Environmental Engineering (IPCBEE). 2015;81(13):74-80.
63. Rod SK, Hansen F, Leipold F, Knochel S. Cold atmospheric pressure plasma treatment of ready-to-eat meat: Inactivation of Listeria innocua and changes in product quality. Food Microbiol. 2012;30(1):233-8.
64. Frohling A, Durek J, Schnabel U, Ehlbeck J, Bolling J, Schluter O. Indirect plasma treatment of fresh pork: Decontamination efficiency and effects on quality attributes. Innovative Food Science & Emerging Technologies. 2012;16:381-90.
65. Tappi S, Gozzi G, Vannini L, Berardinelli A, Romani S, Ragni L, et al. Cold plasma treatment for fresh-cut melon stabilization. Innovative Food Science & Emerging Technologies. 2016;33:225-33.
66. Govaert M, Smet C, Walsh JL, Van Impe JFM. Dual-Species Model Biofilm Consisting of Listeria monocytogenes and Salmonella Typhimurium: Development and Inactivation With Cold Atmospheric Plasma (CAP). Front Microbiol. 2019;10.
67. Scholtz V, Pazlarova J, Souskova H, Khun J, Julak J. Nonthermal plasma - A tool for decontamination and disinfection. Biotechnol Adv. 2015;33(6):1108-19.
68. Li YF, Shimizu T, Zimmermann JL, Morfill GE. Cold Atmospheric Plasma for Surface Disinfection. Plasma Process Polym. 2012;9(6):585-9.
69. Pankaj SK, Bueno-Ferrer C, Misra NN, Milosavljevic V, O'Donnell CP, Bourke P, et al. Applications of cold plasma technology in food packaging. Trends Food Sci Tech. 2014;35(1):5-17.
70. Schnabel U, Andrasch M, Weltmann KD, Ehlbeck J. Inactivation of Microorganisms in Tyvek Packaging by Microwave Plasma Processed Air. Global Journal of Biology Agriculture and Health Science. 2015;4(1):185-92.
71. Jung S, Kim HJ, Park S, Yong HI, Choe JH, Jeon HJ, et al. Color Developing Capacity of Plasma-treated Water as a Source of Nitrite for Meat Curing. Korean J Food Sci An. 2015;35(5):703-6.
72. Yong HI, Park J, Kim HJ, Jung S, Park S, Lee HJ, et al. An innovative curing process with plasma-treated water for production of loin ham and for its quality and safety. Plasma Process Polym. 2018;15(2).
73. Thirumdas R, Kothakota A, Annapure U, Siliveru K, Blundell R, Gatt R, et al. Plasma activated water (PAW): Chemistry, physico-chemical properties, applications in food and agriculture. Trends Food Sci

Tech. 2018;77:21-31.
74. Patange A, Boehm D, Ziuzina D, Cullen PJ, Gilmore B, Bourke P. High voltage atmospheric cold air plasma control of bacterial biofilms on fresh produce. Int J Food Microbiol. 2019;293:137-45.
75. Doijad SP, Barbuddhe SB, Garg S, Poharkar KV, Kalorey DR, Kurkure NV, et al. Biofilm-Forming Abilities of Listeria monocytogenes Serotypes Isolated from Different Sources. Plos One. 2015;10(9).
76. Ziuzina D, Han L, Cullen PJ, Bourke P. Cold plasma inactivation of internalised bacteria and biofilms for Salmonella enterica serovar Typhimurium, Listeria monocytogenes and Escherichia coli. Int J Food Microbiol. 2015;210:53-61.
77. Ziuzina D, Patil S, Cullen PJ, Boehm D, Bourke P. Dielectric Barrier Discharge Atmospheric Cold Plasma for Inactivation of Pseudomonas aeruginosa Biofilms. Plasma Medicine. 2014;4(1-4):137-52.
78. Srey S, Park SY, Jahid IK, Ha SD. Reduction effect of the selected chemical and physical treatments to reduce L-monocytogenes biofilms formed on lettuce and cabbage. Food Res Int. 2014;62:484-91.
79. Bourke P, Ziuzina D, Han L, Cullen PJ, Gilmore BF. Microbiological interactions with cold plasma. J Appl Microbiol. 2017;123(2):308-24.
80. Gilmore BF, Flynn PB, O'Brien S, Hickok N, Freeman T, Bourke P. Cold Plasmas for Biofilm Control: Opportunities and Challenges. Trends Biotechnol. 2018;36(6):627-38.
81. Vu B, Chen M, Crawford RJ, Ivanova EP. Bacterial Extracellular Polysaccharides Involved in Biofilm Formation. Molecules. 2009;14(7):2535-54.
82. Molobela IP, Cloete TE, Beukes M. Protease and amylase enzymes for biofilm removal and degradation of extracellular polymeric substances (EPS) produced by Pseudomonas fluorescens bacteria. Afr J Microbiol Res. 2010;4(14):1515-24.
83. Simoes M, Carvalho H, Pereira MO, Vieira MJ. Studies on the behaviour of Pseudomonas fluorescens biofilms after ortho-phthalaldehyde treatment. Biofouling. 2003;19(3):151-7.
84. Colagiorgi A, Di Ciccio P, Zanardi E, Ghidini S, Ianieri A. A Look inside the Listeria monocytogenes Biofilms Extracellular Matrix. Microorganisms. 2016;4(3).
85. Evans LV. Biofilms: Recent advances in their study and control. CRC Press Taylor & Francis e-Libary. 2005:490.
86. Flemming HC, Wingender J. The biofilm matrix. Nat Rev Microbiol. 2010;8(9):623-33.
87. Allison DG. The biofilm matrix. Biofouling. 2003;19(2):139-50.

Figures

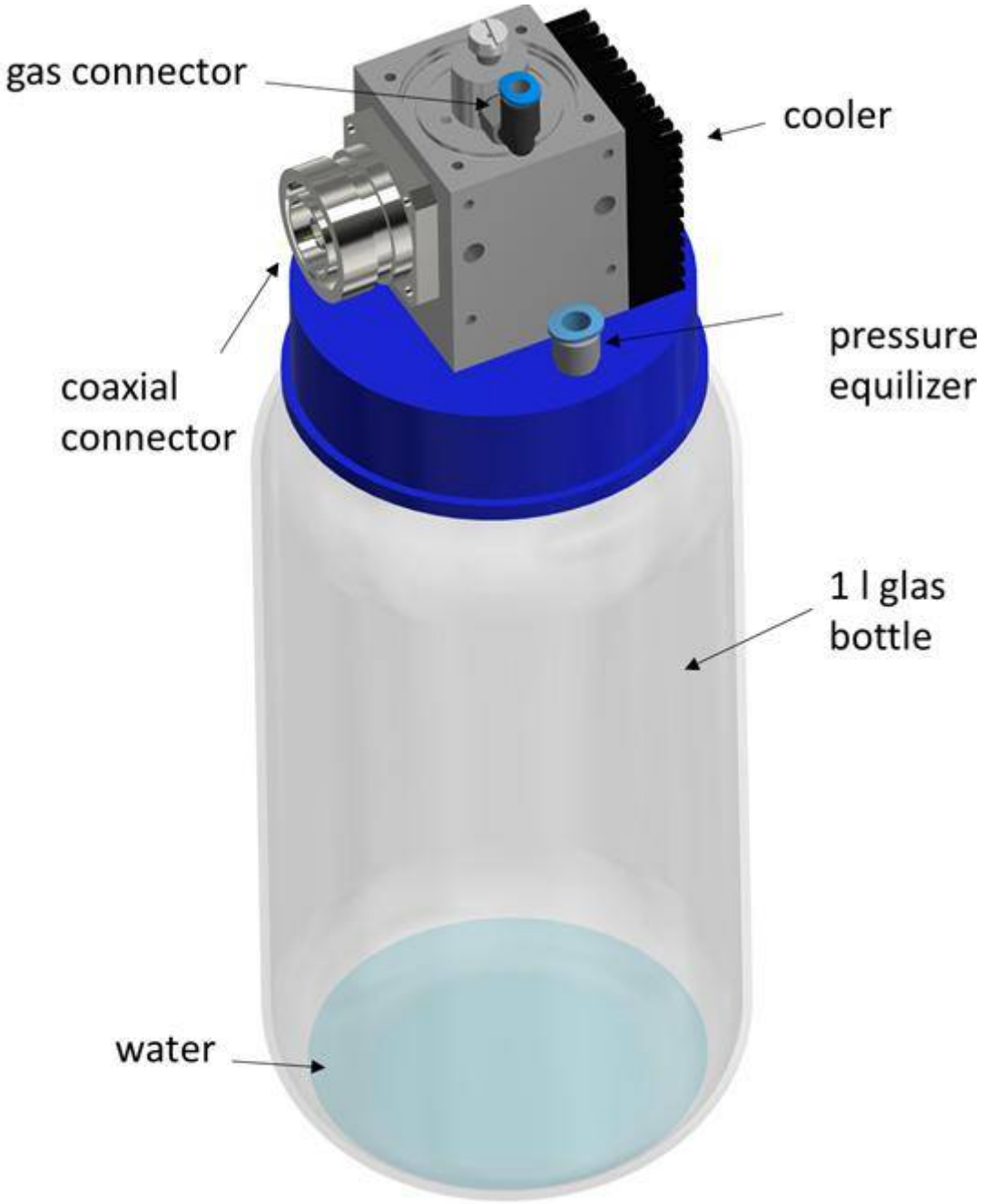

Figure 1

schematic illustration of the MidiPLexc Schematic illustration of the MidiPLexc with 1 l glas bottle attached to the bottle adapter of the plasma source modified according to (39).

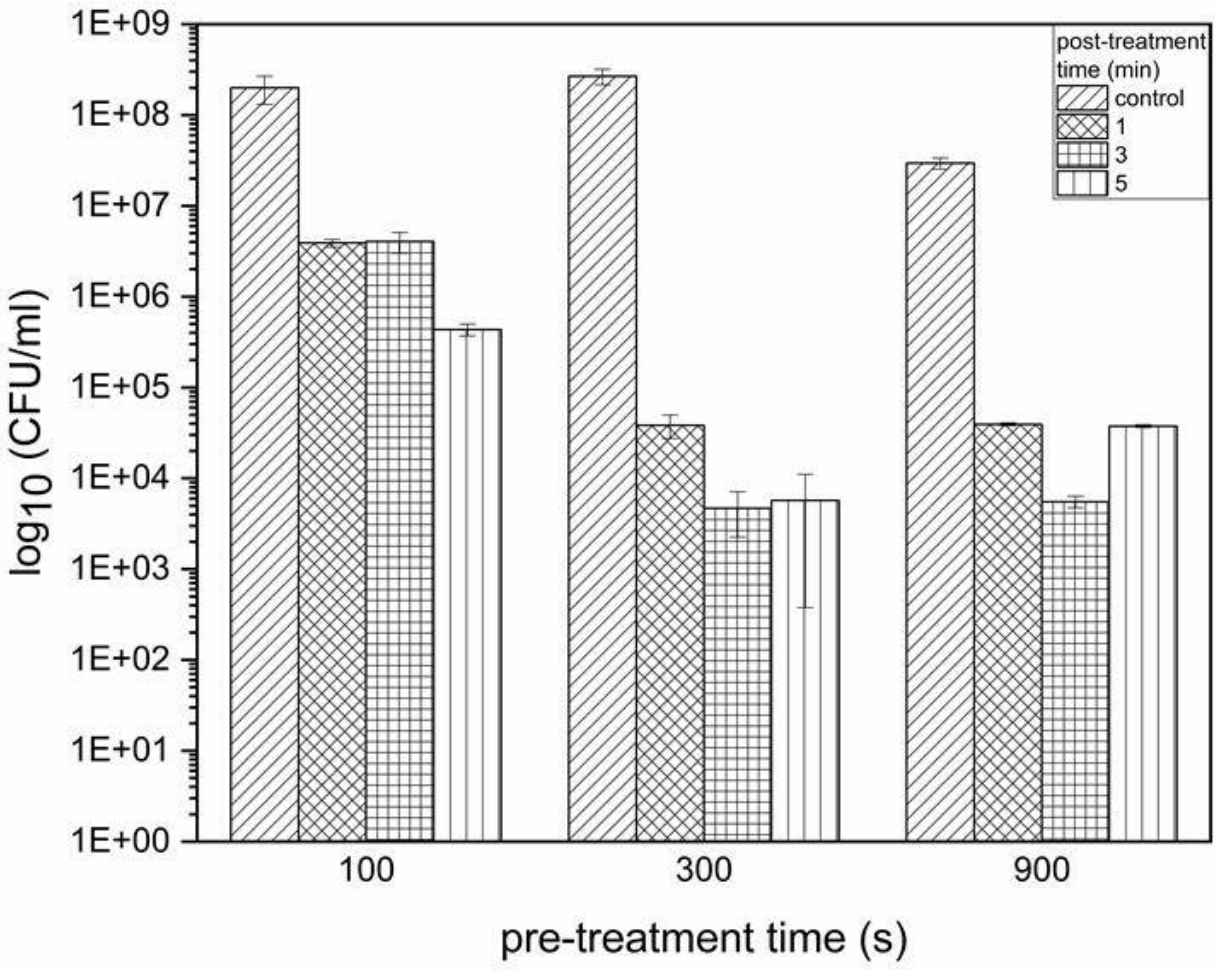

Figure 2

Colony-forming units of Listeria monocytogenes biofilms after PTW treatment The graph show the reduction in the colony-forming units (CFUs) after plasma treatment of the biofilms. The grouped bar chart show at the x-axis the water treatment time with the Midiplexc (pretreatment time) and the bars show the biofilm treatment time with the plasma-treated water (post treatment time). The experiment was performed in four independent experiments with three technical replicates each.

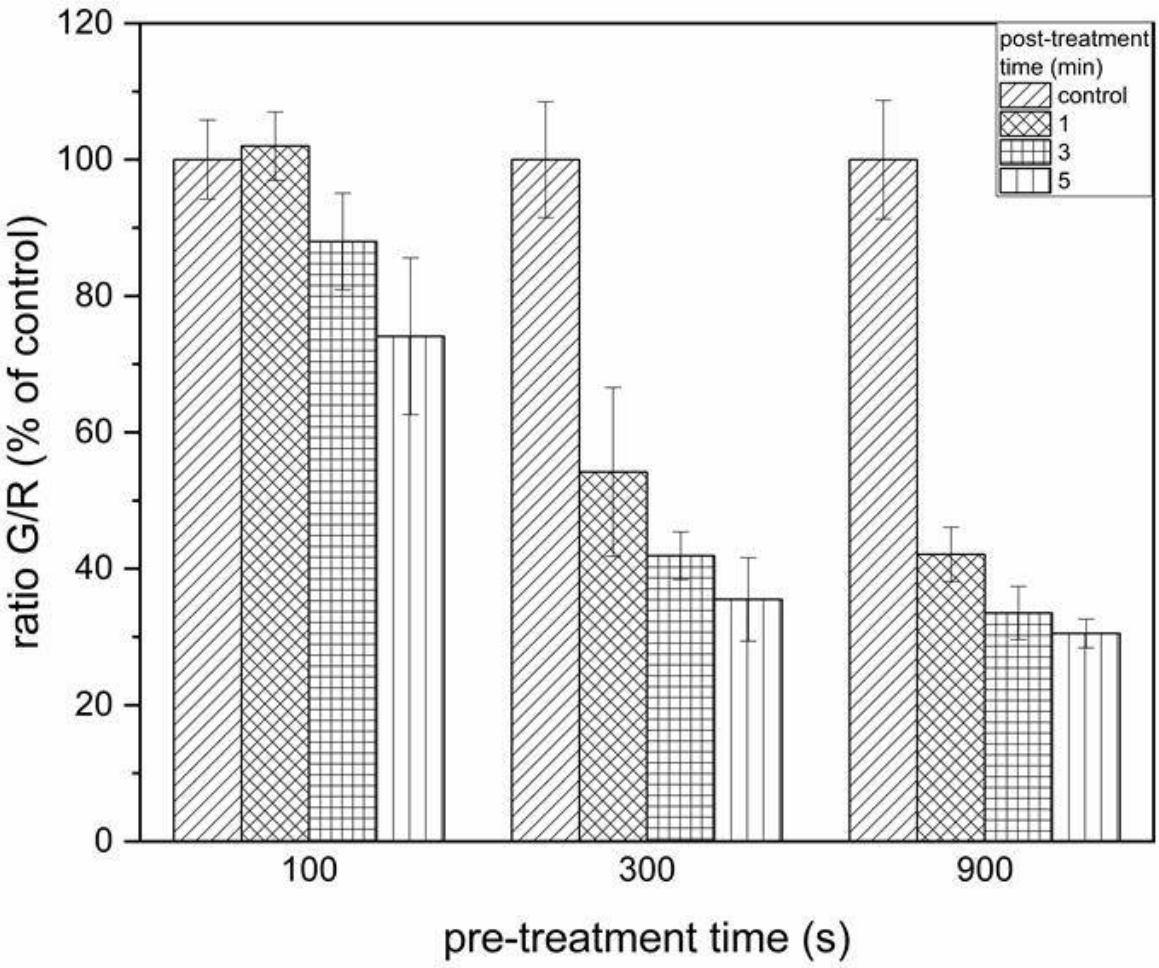

Figure 3

Live/Dead assay of Listeria monocytogenes biofilms after PTW treatment The graph show the reduction in the ratio G/R after treatment of the biofilms with the plasma-treated water. The grouped bar chart show at the x-axis the water treatment time with the Midiplexc (pretreatment time) and the bars show the biofilm treatment time with the plasma-treated water (post-treatment time). The experiment was performed in four independent experiments with three technical replicates each.

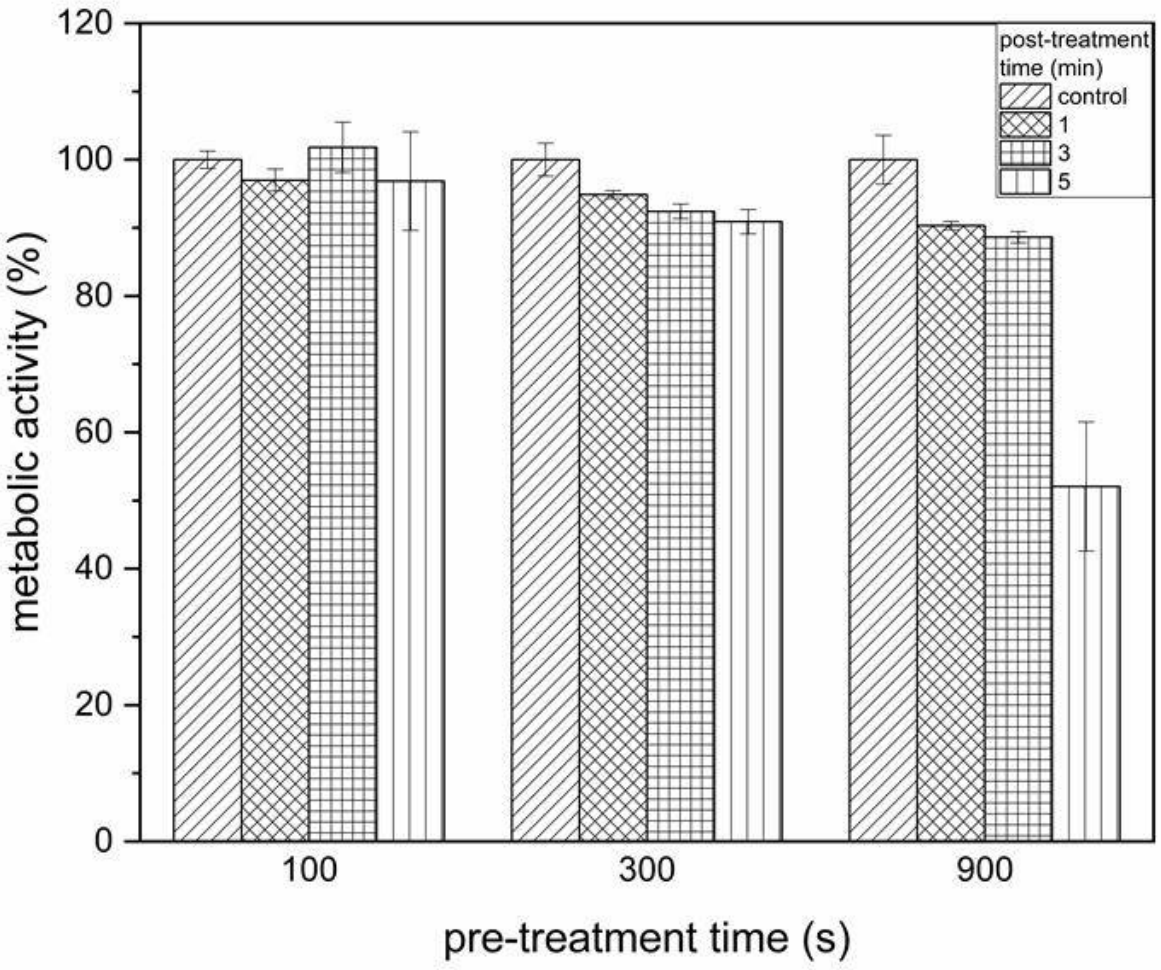

Figure 4

XTT assay of Listeria monocytogenes biofilms after PTW treatment The graph show the reduction in the metabolic activity after treatment of the biofilms with the plasma-treated water. The grouped bar chart show at the x-axis the water treatment time with the Midiplexc (pretreatment time) and the bars show the biofilm treatment time with the plasma-treated water (post-treatment time). The experiment was performed in four independent experiments with three technical replicates each.

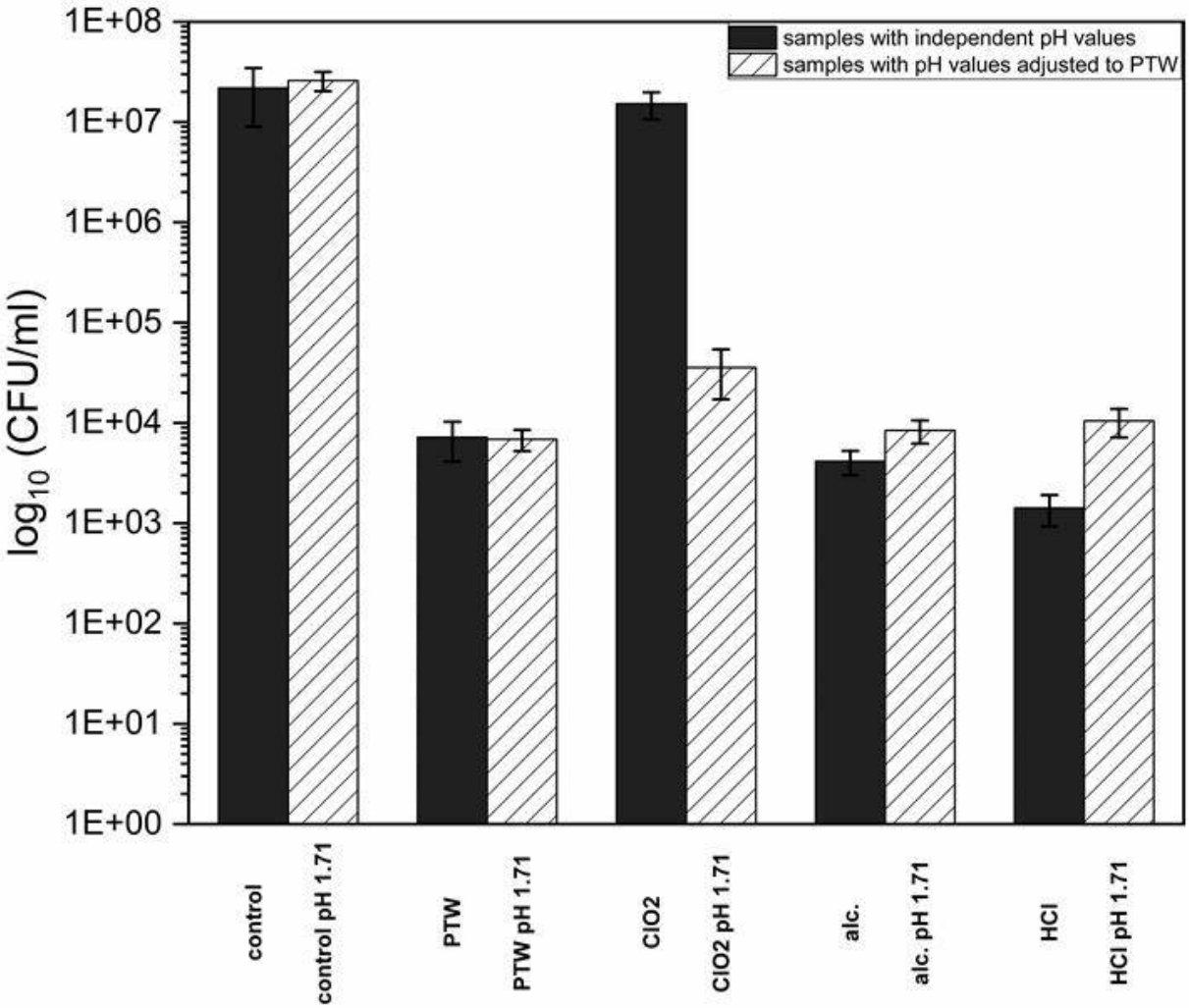

Figure 5

Colony-forming units of Listeria monocytogenes biofilms after treatment with different chemicals The graph show the reduction in the colony-forming units of Listeria monocytogenes biofilms after treatment with different chemicals often used in the food-production industry. The effects of plasma-treated water (PTW), chlorine dioxide (ClO2), 70 % alcohol and fuming hydrochloric acid were compared. The black bars show the effect of each substance at its own pH value and the striped bars show the effect of the substances when their pH value is adjusted to that of the PTW.

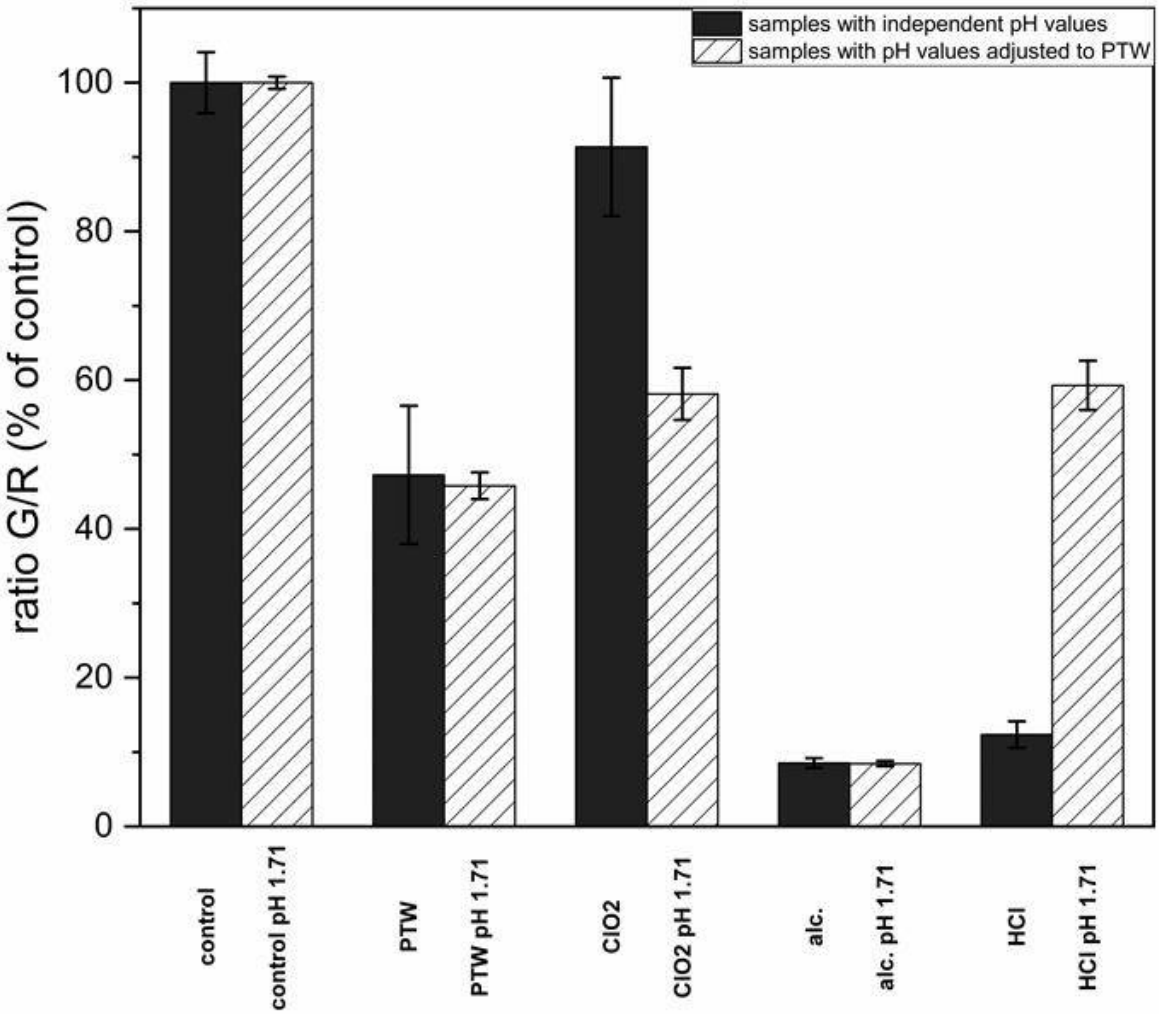

Figure 6

Live/Dead assay of Listeria monocytogenes biofilms after treatment with different chemicals The graph show the reduction in the Ratio G/R of Listeria monocytogenes biofilms after treatment with different chemicals often used in the food-production industry. The effects of plasma-treated water (PTW), chlorine dioxide (ClO2), 70 % alcohol and fuming hydrochloric acid were compared. The black bars show the effect of each substance at its own pH value and the striped bars show the effect of the substances when their pH value is adjusted to that of the PTW.

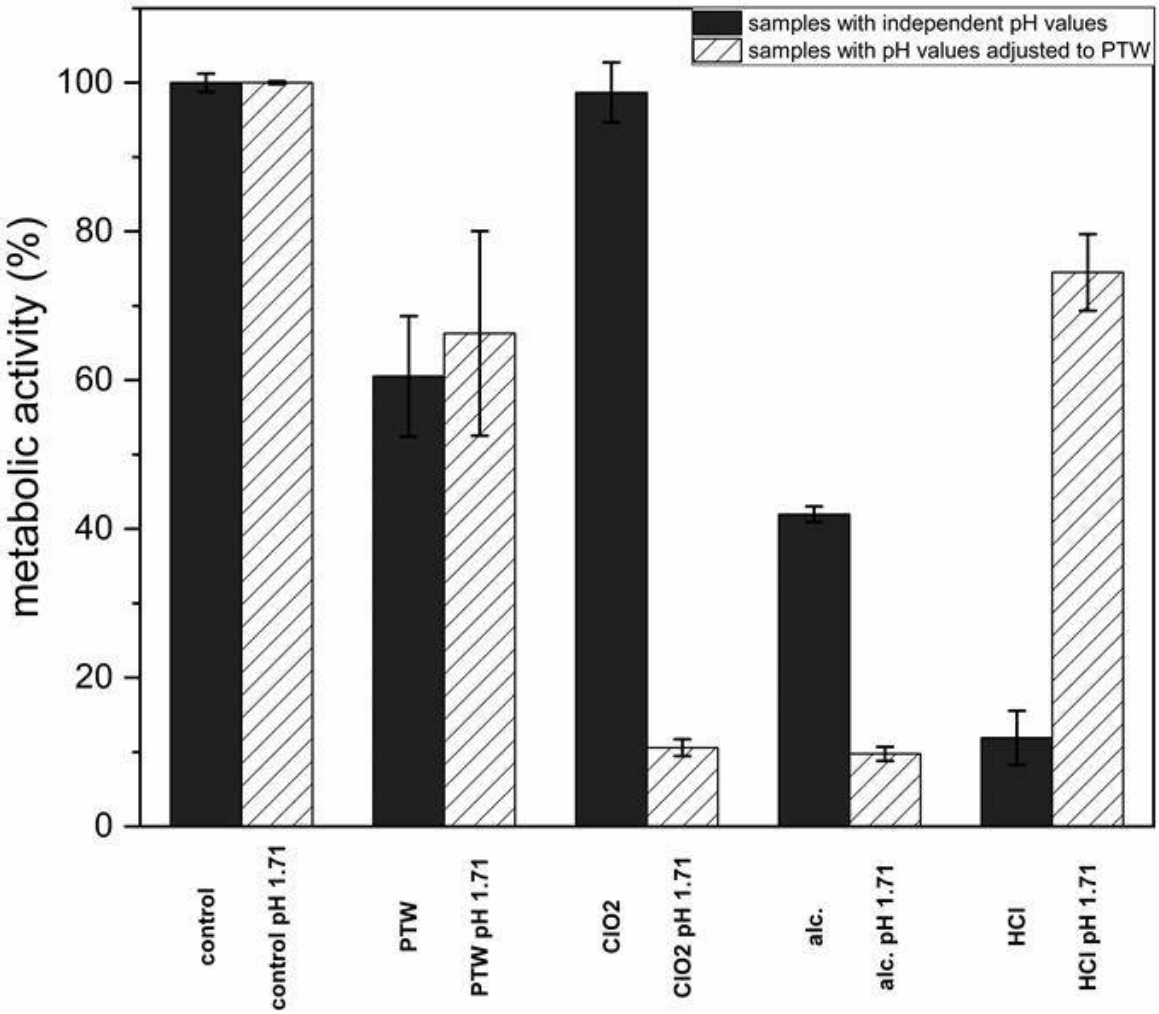

Figure 7

XTT assay of Listeria monocytogenes biofilms after treatment with different chemicals The graph show the reduction in the metabolic activity of Listeria monocytogenes biofilms after treatment with different chemicals often used in the food-production industry. The effects of plasma-treated water (PTW), chlorine dioxide (ClO2), 70 % alcohol and fuming hydrochloric acid were compared. The black bars show the effect of each substance at its own pH value and the striped bars show the effect of the substances when their pH value is adjusted to that of the PTW.

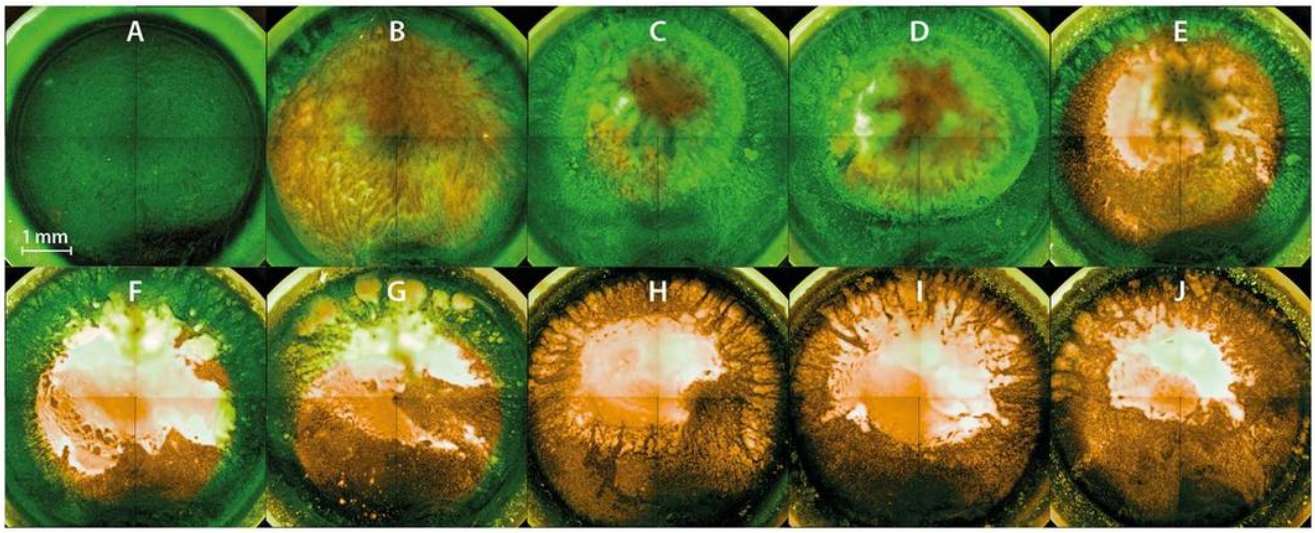

Figure 8

Fluorescence microscopy of Listeria monocytogenes biofilms after PTW treatment The images show inverse footage of the biofilms. The pretreatment time defines the time period in which the water came into contact with the plasma gas. The post-treatment time represents the period of time where the PTW came into contact with the biofilm. The biofilms are stained with SYTO9 (green) for living cells and propidium iodide (red) for dead cells. A) Control biofilm B) 100 s pretreatment, 1 min post treatment C) 100 s pretreatment time, 3 min post-treatment time D) 100 s pretreatment, 5 min post treatment E) 300 s pretreatment, 1 min post treatment F) 300 s pretreatment, 3 min post treatment G) 300 s pretreatment, 5 min post treatment H) 900 s pretreatment, 1 min post treatment I) 900 s pretreatment, 3 min post treatment J) 900 s pretreatment, 5 min post treatment.

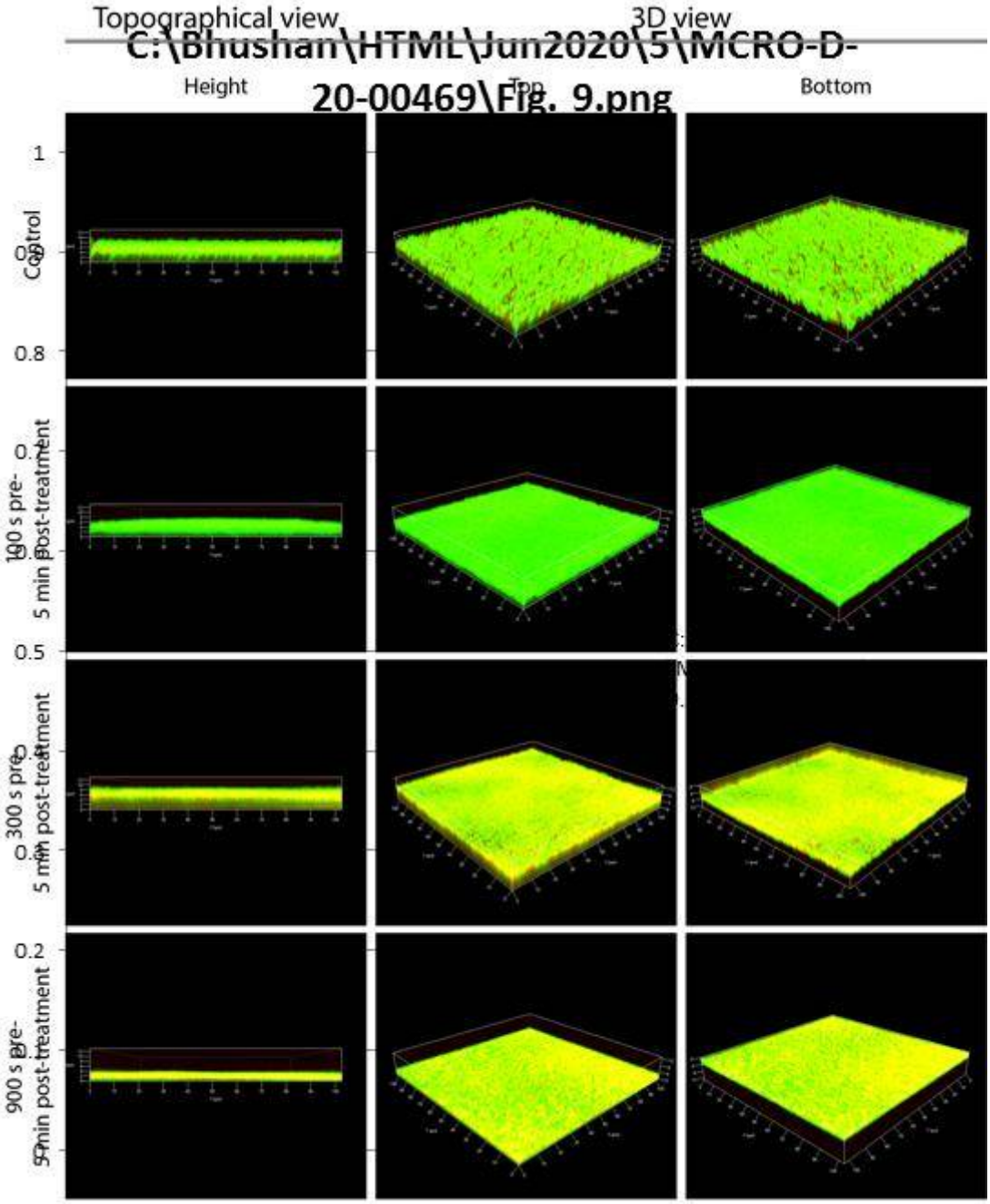

Figure 9

Confocal laser scanning microscopy (CLSM) of Listeria monocytogenes biofilms after PTW treatment
The images show Listeria monocytogenes biofilms with and without treatment with plasma treated water (PTW). Left panels show a topographical view of the biofilm layer (height view of the biofilms in µm). Central and right panels show 3D images with a top and a bottom view of the biofilms, respectively. The pretreatment time is the treatment time of the water by the plasma source (MidiPLexc) and the post-treatment time is the contact time of the PTW with the biofilm. For each biofilm, an area of 100 × 100 µm is visualized.

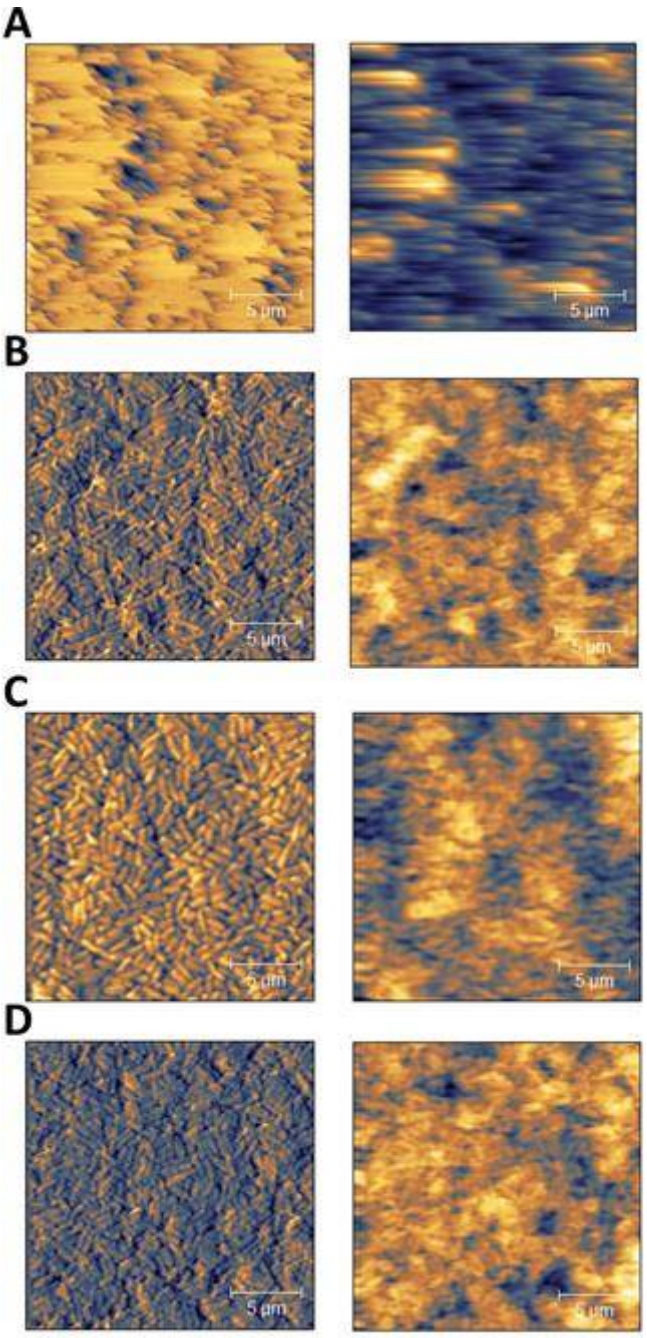

Figure 10

Atomic-force microscopy (AFM) of Listeria monocytogenes biofilms after PTW treatment Atomic force microscopy (AFM) images of Listeria monocytogenes biofilms. Left) topographical images right) error images. The pretreatment time defines the time period in which the water came into contact with the plasma gas. The post-treatment time represents the period of time, where the PTW came into contact with the biofilm. A) Control biofilm B) 100 s pretreatment, 5 min post treatment C) 300 s pretreatment, 5 min post treatment D) 900 s pretreatment, 5 min post treatment.

Supplementary Files

This is a list of supplementary files associated with this preprint. Click to download.

- l.m.control3D2.wmv
- l.m.900s3D2.wmv